PHYSICAL REVIEW B **81**, 140404(R) (2010)

Reverse Doppler effect of magnons with negative group velocity scattered from a moving Bragg grating

A. V. Chumak,[1] P. Dhagat,[2] A. Jander,[2] A. A. Serga,[1] and B. Hillebrands[1]
[1]*Fachbereich Physik and Forschungszentrum OPTIMAS, Technische Universität Kaiserslautern, 67663 Kaiserslautern, Germany*
[2]*School of Electrical Engineering and Computer Science, Oregon State University, Corvallis, Oregon 97331, USA*
(Received 11 March 2010; published 16 April 2010)

We demonstrate experimentally and theoretically the reverse Doppler effect when magnons with negative group velocity are reflected off a moving Bragg grating. This grating, which represents a moving magnonic crystal, is created in an yttrium-iron-garnet film by the periodic strain induced by a traveling surface acoustic wave. As reflection occurs from a crystal rather than from a single reflecting surface, the wave number of the scattered wave is strictly determined by a momentum conservation law. Magnons scattered from the approaching (receding) magnonic crystal are found to be shifted down (up) in frequency. This result, together with an earlier report of reverse Doppler shift from moving sources [D. D. Stancil *et al.*, Phys. Rev. B, **74**, 060404(R) (2006)], establishes that the reverse Doppler effect is a universal phenomenon in systems with negative group velocity and not restricted to left-handed materials.

DOI: 10.1103/PhysRevB.81.140404 PACS number(s): 75.30.Ds, 63.20.kk, 85.70.Ge

The Doppler effect (or Doppler shift) is a well-known phenomenon. It describes the frequency shift a wave experiences if it is emitted from a moving source or reflected off of a moving boundary.[1,2] The effect is widely used in radar systems, laser vibrometry and astronomical observations.

In left-handed media[3] the reverse (or anomalous) Doppler effect has been reported,[3–8] where waves are reflected from an approaching (receding) boundary with lowered (increased) frequency in contrast to everyday experience in acoustics. The common explanation is that in left-handed media the group and phase velocities of the waves are in opposite directions.[9] The frequency at which the reflector produces waves is determined by the rate at which it encounters the wave crests from the source. For a wave group approaching the reflector in a left-handed medium, the wave crests are actually moving away from the reflector. Thus, the reflector encounters fewer (more) crests per second if it is moving toward (away from) the source than if it were stationary, resulting in a lower (higher) frequency of the reflected wave.

The reverse Doppler effect has also been observed in media which are not left-handed but show a negative group velocity due to negative slope in the dispersion curve (frequency decreases with increasing wave vector).[8] In that work, a moving microwave antenna was used to excite spin waves in a yttrium-iron-garnet (YIG) film. Due to their negative group velocity the spin waves generated by the moving antenna experienced a reverse Doppler shift.

However, it was not clear that the effect is universal. To show the latter, demonstration of a reverse frequency shift upon reflection off of a moving target was lacking. Moreover, there is a lack of knowledge about the manifestation of the reverse Doppler effect in cases where the reflection is from a periodic medium with reflection conditions strictly determined by a momentum-conservation law. Such systems in the form of photonic, magnonic, and sonic crystals (see, for example, Refs. 6 and 9–11) are of widespread contemporary scientific interest.

In this Rapid Communication, we report the experimental observation of a reverse Doppler effect on waves with negative group velocity scattered from a Bragg grating formed by a moving one-dimensional magnonic crystal. Magnetostatic spin waves traveling in a thin-film magnetic material, saturated by a magnetic field along the direction of propagation, are known to have a negative slope of the dispersion curve. We show, that such waves, termed backward volume magnetostatic waves (BVMSW),[12] show a reverse Doppler effect when reflected off of a moving Bragg grating created by a propagating surface acoustic wave. These results are interesting for both fundamental research on linear and nonlinear wave dynamics, magnon-phonon interactions, and for signal processing in the microwave frequency range. Microwave devices such as frequency shifters, adaptive matched filters, and phonon detectors may be conceived using inelastic scattering of spin waves on acoustic waves.

The experiments were performed using 6-μm-thick YIG film which was epitaxially grown on 500-μm-thick, (111)-oriented gadolinium gallium garnet (GGG) substrate. The substrate was cut into strips approximately 3-mm wide and 2-cm long. The conditions for BVMSW propagation were established by applying an in-plane external bias magnetic field of H_0=1630 Oe along the length of the YIG strip and parallel to the direction of spin-wave propagation (see Fig. 1). BVMSWs were excited and detected in the YIG film using microwave stripline antennas spaced 8 mm apart

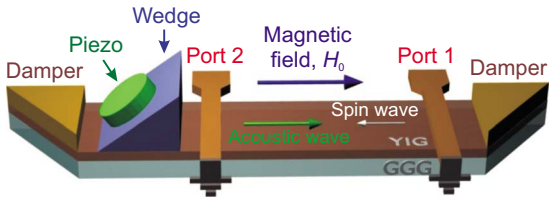

FIG. 1. (Color online) Experimental setup. Spin waves are excited and detected in the YIG film by stripline antennas (Port 1 and Port 2). The surface acoustic wave providing the Bragg grating for spin-wave scattering is excited on the YIG/GGG sample by a piezoelectric quartz crystal and an acrylic wedge transducer.

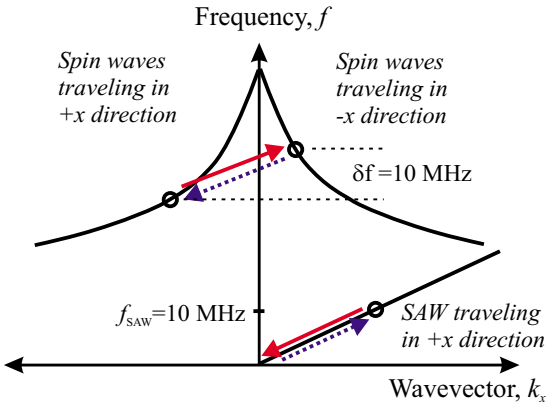

FIG. 2. (Color online) Schematic of dispersion curves for BVMSW and SAW. Circles indicate the waves that participate in Bragg scattering. Red solid arrows show the process of scattering of BVMSW on *copropagating* SAW resulting in spin waves shifted up in frequency while a phonon is annihilated. Blue dashed arrows show the process of scattering of BVMSW on *counterpropagating* SAW with the resulting spin-wave frequency shifted down while a phonon is generated.

(shown as Port 1 and Port 2 in Fig. 1). The spin waves were generated by driving the antennas with the microwave source of a network analyzer (model Agilent N5230C). The microwave signal power, at 1 mW, was low enough to avoid nonlinear processes. The microwave frequency was swept through the range 6.4–6.6 GHz. Simultaneously, surface acoustic waves (SAWs) were launched to propagate along the same path on the YIG/GGG sample. Longitudinal compressional waves at frequency f_{SAW}=10 MHz were generated using a piezoelectric quartz crystal and coupled to surface modes in the YIG/GGG with an acrylic wedge transducer.[13] The wedge was machined to 51° for most efficiently transforming bulk acoustic waves into surface acoustic waves. A transformer and resonant circuit were used for impedance matching between the 50 Ω source and the piezoelectric crystal. The ends of the YIG/GGG sample were cut at a 45° angle and coated with a silicone acoustic absorber to avoid reflections (see Fig. 1).

The acoustic waves interact with the spin waves through the magnetostrictive effect in the magnetic material.[14,15] The strain induced by the acoustic wave periodically modulates the magnetic properties of the film, effectively producing a traveling magnonic crystal off which the spin waves are reflected. Figure 2 shows schematically the dispersion curves for both the BVMSW and SAW. One can see that the group velocity of BVMSW, as determined from the slope of the dispersion curve, is negative for positive wave vectors and vice versa. Thus, points on the BVMSW curve to the left of the axis represent waves propagating or carrying energy to the right from Port 2 to Port 1. Conversely, spin waves propagating to the left from Port 1 to Port 2 appear on the right side of the plot. The surface acoustic waves have a normal, linear-dispersion relation: SAW traveling to the right from the prism are indicated by points on the right side of the plot.

The scattering process of spin waves on the acoustic waves must conserve energy and momentum. Figure 2 shows

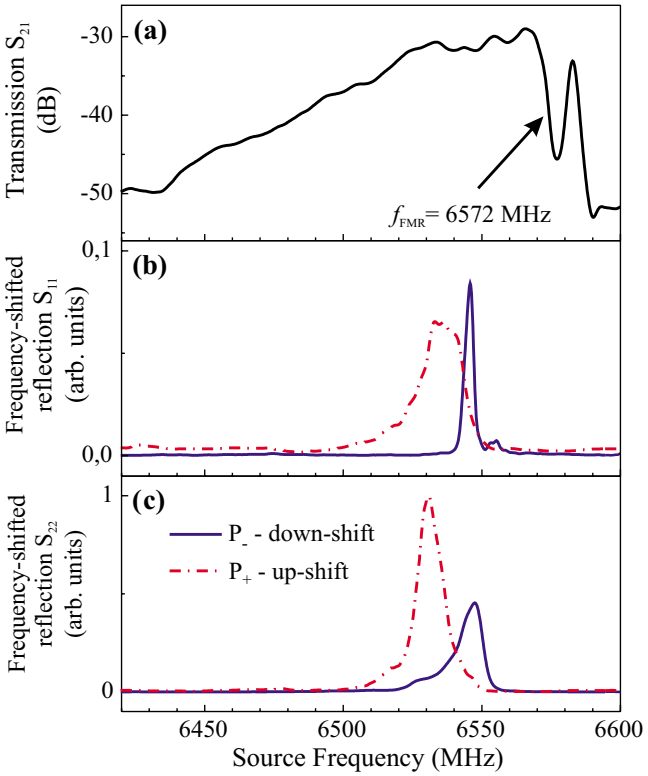

FIG. 3. (Color online) (a) BVMSW transmission characteristic for the YIG film. [(b) and (c)] The reflection characteristics for Port 1 and Port 2, respectively. The solid blue curve, P_-, is for the detector frequency set 10 MHz below the source frequency. The dashed red curve, P_+, is for the detector frequency set 10 MHz above the source frequency. In each case, the frequency axis is the swept source frequency.

schematically the transitions allowed by the conservation laws. The annihilation of a phonon (red solid arrows in Fig. 2) corresponds to the generation of a magnon of higher frequency and traveling in the opposite direction of the original spin wave. It is clear that for the experimental setup shown in Fig. 1, this interaction can be realized only for the spin wave which propagates in the $+x$ direction, i.e., in the same direction as the SAW. One can see that the Doppler effect is reversed since the reflected spin wave has higher frequency. Another process is realized with the generation of the phonon (blue dashed arrows in Fig. 2), which corresponds to the generation of a magnon of lower frequency traveling in the opposite direction of the original spin wave. This process takes place between counterpropagating spin and acoustic waves. The Doppler shift, δf, is equal to the SAW frequency in both cases.

Figure 3(a) shows the experimentally measured BVMSW transmission characteristic for the YIG film as determined from the S_{21} parameter (power received at Port 2 relative to the power delivered to Port 1). The spin-wave transmission band is bounded above by the ferromagnetic resonance frequency and below by the antenna excitation efficiency. It has a maximum just below ferromagnetic resonance frequency (the theoretically calculated f_{FMR}=6572 MHz).

Figure 3(b) shows the reflection characteristics for Port 1 (S_{11} parameter) due to spin waves generated at Port 1 being

reflected back to the same antenna. The Doppler-shifted frequencies were measured by tuning the network analyzer to detect signals at frequencies offset by plus and minus 10 MHz (i.e., $\pm f_{\mathrm{SAW}}$) from the swept source frequency. Similarly, the reflection characteristics for Port 2 are shown in Fig. 3(c). In each case, the frequency axis is the swept source frequency.

One can clearly see from Fig. 3(b) that both up-shifted (P_+ signal in figure) and down-shifted (P_- signal) frequencies exist for the reflected spin waves. The reason is as follows: with the microwave signal applied to Port 1, the antenna excites spin waves propagating outward in both directions from the antenna. The spin waves propagating to the left, toward the acoustic source, encounter approaching surface acoustic waves and are partially scattered back toward the source antenna with a reverse Doppler shift down in frequency. The spin waves propagating to the right, away from the acoustic source, encounter receding acoustic waves and are scattered back with an up-shift in frequency due to the reverse Doppler effect.

The allowed transitions shown in Fig. 2 are equivalent to the Bragg reflection conditions. For frequencies meeting these conditions, the reflected spin-wave power is maximized and this is the reason why the reflected spin-wave signal is much narrower in the frequency space in comparison to the transmission characteristic S_{21}. The peaks in the P_+ and P_- curves correspond to the phonon annihilating up-shift and phonon generating down-shift processes, respectively. The down-shift process must start at a higher spin-wave-source frequency and, in the reverse transition, the up-shift process must start from a lower original spin-wave frequency. Thus, the difference in source frequency for the up-shift and down-shift process, δf, should be equal to the SAW frequency, f_{SAW}. This is seen in the experimental results shown in Fig. 3(b): the source frequency at which the P_+ signal reaches a maximum is 10 MHz lower as compared to the P_- signal. The peak of the down-shifted reflection is larger and narrower because the path length over which the acoustic and spin waves can interact is approximately two times longer on the left side of the antenna. Although both up-shifted and down-shifted signals are present in the experimental results, it is clear from the relative amplitudes that the up-shifted signal is due to the copropagating waves, verifying the reverse Doppler effect.

The reflection characteristics for Port 2 are presented in Fig. 3(c). One can see that for Port 2, the up-shifted reflection is stronger because the rightward propagating spin waves (which reflect off of receding acoustic waves) have a longer interaction path length. Note the difference in the scale between Figs. 3(b) and 3(c); the Port 2 signals are stronger because the acoustic amplitude is larger near the source. Similar to Port 1 results, the positions of the peaks differ by approximately f_{SAW}. The frequency difference between the maxima in P_- and P_+ signals is $\delta f_1 = 10$ MHz and $\delta f_2 = 15$ MHz for Port 1 and Port 2, respectively. The discrepancy in δf_2 from the expected 10 MHz is likely due to part of the interaction occurring under the wedge: here, the SAW velocity (and wavelength correspondingly) differs from that in the unloaded YIG film. Thus, the spin-wave frequencies at which the Bragg conditions are met are different for the copropagating and counterpropagating cases. It should be noted that the actual Doppler frequency shift in the reflected spin wave is exactly 10 MHz in both cases, as determined by the detector frequency offset.

To construct a simple and representative theoretical model, we consider the BVMSW dispersion relation to be nearly linear for small wave numbers ($kd \ll 1$, where d is the thickness of the YIG film). Thus, using formula (4.96b) in Ref. 16 we can write the spin-wave frequency as

$$f_{\mathrm{SW}}(k) = f_{\mathrm{FMR}} + \frac{v_{\mathrm{SW}}}{2\pi} \cdot k,$$

where

$$v_{\mathrm{SW}} = 2\pi \frac{\partial f_{\mathrm{SW}}}{\partial k} = -\frac{\pi}{2} \frac{f_{\mathrm{H}} f_{\mathrm{M}}}{f_{\mathrm{FMR}}} d$$

is the group velocity of BVMSW. Here $f_{\mathrm{H}} = \gamma H_0$, $f_{\mathrm{M}} = 4\pi\gamma M_0$, $\gamma = 2.8$ MHz/Oe is the gyromagnetic ratio, M_0 is the saturation magnetization, and $f_{\mathrm{FMR}} = \sqrt{f_{\mathrm{H}}(f_{\mathrm{H}} + f_{\mathrm{M}})}$.

The dispersion relation for the SAW is nearly linear with $f_{\mathrm{SAW}}(k) = v_{\mathrm{SAW}} \cdot k$, where v_{SAW} is the phase and group velocity of the acoustic wave. Fulfilling laws of energy and momentum conversation by the transitions indicated in Fig. 2, a simple equation can be derived for the initial spin-wave frequencies f_+ and f_- which correspond to the maxima of P_+ and P_-

$$f_{\pm} = f_{\mathrm{FMR}} - \frac{f_{\mathrm{SAW}}}{2}\left(\frac{|v_{\mathrm{SW}}|}{v_{\mathrm{SAW}}} \pm 1\right).$$

Using $4\pi M_0 = 1750$ G for the YIG film, BVMSW group velocity $v_{\mathrm{SW}} = -3.2$ cm/μs, and SAW velocity $v_{\mathrm{SAW}} = 0.5$ cm/μs this equation gives the values for $f_+ = 6535$ MHz and $f_- = 6545$ MHz which is in good agreement with the experimental data plotted in Fig. 3.

In conclusion, we have observed the reverse Doppler effect in backward spin waves reflected off a traveling Bragg grating formed by surface acoustic waves. As the waves are scattered from a propagating grating rather than a single reflecting surface, a special condition is placed on the wave number of the scattered wave and reflection is observed in very narrow frequency range. Both possible situations were analyzed: the scattering of BVMSW from copropagating and counterpropagating SAW. It was shown that the frequencies of scattered spin waves in both cases were shifted by the frequency of SAW according to the reverse Doppler effect. The results are in good agreement with the theoretical analysis based on the dispersion curves of spin waves and acoustic waves. The results show that, as well as being measurable in systems with moving emitters and receivers (Ref. 8), the reverse Doppler effect is a general phenomenon in materials with a negative group velocity and can be observed in systems with moving reflectors.

This work was partially supported by the DFG under Grant No. SE 1771/1-1 and NSF under Grant No. ECCS 0645236. Special acknowledgments to G. A. Melkov for valuable discussions.

[1] C. Doppler, Abh. Königlich Böhmischen Ges. Wiss. **2**, 465 (1843).
[2] C. H. Papas, *Theory of Electromagnetic Wave Propagation* (McGraw-Hill, New York, 1965).
[3] V. E. Pafomov, Sov. Phys. JETP **36**, 1853 (1959).
[4] V. G. Veselago, Fiz. Tverd. Tela **8**, 3571 (1966).
[5] N. Seddon and T. Bearpark, Science **302**, 1537 (2003).
[6] E. J. Reed, M. Soljacic, and J. D. Joannopoulos, Phys. Rev. Lett. **91**, 133901 (2003).
[7] K. Leong, A. Lai, and T. Itoh, Microwave Opt. Technol. Lett. **48**, 545 (2006).
[8] D. D. Stancil, B. E. Henty, A. G. Cepni, and J. P. Van't Hof, Phys. Rev. B **74**, 060404(R) (2006).
[9] V. G. Veselago, Usp. Fiz. Nauk **92**, 517 (1967).
[10] A. V. Chumak, A. A. Serga, B. Hillebrands, and M. P. Kostylev, Appl. Phys. Lett. **93**, 022508 (2008).
[11] T. Miyashita, Meas. Sci. Technol. **16**, R47 (2005).
[12] R. W. Damon and J. R. Eshbach, Phys. Chem. Solids **19**, 308 (1961).
[13] S. Hanna, G. Murphy, K. Sabetfakhri, and K. Stratakis, *IEEE 1991 Ultrasonics Symposium Proceedings*, edited by B. R. McAvoy (IEEE, New York, 1990), Vol. 1, p. 209.
[14] S. M. Hanna and G. P. Murphy, IEEE Trans. Magn. **24**, 2814 (1988).
[15] Yu. V. Gulyaev and S. A. Nikitov, Sov. Phys. Solid State **26**, 1589 (1984).
[16] D. D. Stancil, *Theory of Magnetostatic Waves* (Springer, New York, 1993).